Preprint
UCRL-JC-143220

Laboratory and Field Measurements of Electrical Resistivity to Determine Saturation and Detect Fractures in a Heated Rock Mass

J. J. Roberts, A. Ramirez, S. Carlson, W. Ralph, B. P. Bonner, and W. Daily

U.S. Department of Energy

Lawrence
Livermore
National
Laboratory

This article was submitted to
Geothermal Resources Council 2001 Annual Meeting, San Diego, California, August 26-29, 2001

April 3, 2001

LABORATORY AND FIELD MEASUREMENTS OF ELECTRICAL RESISTIVITY TO DETERMINE SATURATION AND DETECT FRACTURES IN A HEATED ROCK MASS

Jeffery J. Roberts, Abelardo Ramirez, Steve Carlson, William Ralph, Brian P. Bonner, and William Daily

Lawrence Livermore National Laboratory
P.O. Box 808, L-201
Livermore, CA 94550
e-mail: roberts17@llnl.gov

Key Words: Electrical Resistivity, Fracture Detection

ABSTRACT

Laboratory measurements of the electrical resistivity of intact and fractured representative geothermal reservoir rocks were performed to investigate the resistivity contrast caused by active boiling and to infer saturation and fracture location in a large-scale field test. Measurements were performed to simulate test conditions with confining pressures up to 100 bars and temperatures to 145°C. Measurements presented are a first step toward making the search for fractures using electrical methods quantitatively. Intact samples showed a gradual resistivity increase when pore pressure was decreased below the phase-boundary pressure of free water, while fractured samples show a larger resistivity change at the onset of boiling. The resistivity change is greatest for samples with the most exposed surface area. Analysis of a field test provided the opportunity to evaluate fracture detection using electrical methods at a large scale. Interpretation of electrical resistance tomography (ERT) images of resistivity contrasts, aided by laboratory derived resistivity-saturation-temperature relationships, indicates that dynamic saturation changes in a heated rock mass are observable and that fractures experiencing drying or resaturation can be identified. The same techniques can be used to locate fractures in geothermal reservoirs using electrical field methods.

INTRODUCTION AND BACKGROUND

The electrical properties of geothermal rocks are important for numerous reasons, including reservoir evaluation, following the effects of production including formation of a steam cap, and tracking injectate. Electrical methods provide the best means to detect and follow fluid movement in the subsurface.

Rock electrical properties are sensitive to factors such as the nature and amount of pore saturant, temperature, pressure (Llera et al., 1990), surface conduction, and microstructural properties such as porosity of the rock matrix. The amount of the pore saturant and its nature (i.e., whether it is liquid water, other fluids, steam, or other gases) and microstructural properties are the most significant factors.

Previous electrical measurements on intact samples from The Geysers (Roberts et al., 2001b) and Awibengkok (Roberts et al., 2000; 2001a), indicate boiling phenomena attributable to vapor-pressure lowering. As fracture properties play a large role in the performance of geothermal reservoirs, we have investigated samples with artificial (propped) fractures in order to assess the electrical signatures that indicate fluid- and steam-filled fractures *in situ*. Electrical methods rely on contrasts in resistivity to locate fractures and to determine if steam is present. These methods include the long-spacing induction tool, cross-well EM and electrical resistance tomography. In this paper we report on progress in utilizing the results from a large-scale field test named the Large Block Test combined with laboratory electrical measurements to quantitatively evaluate changing saturation and fracture location in a rock mass heated to above boiling.

THE LARGE BLOCK TEST

Background and Instrumentation

The Large Block Test (LBT) was a multi-disciplinary field-scale experiment performed by researchers from Lawrence Livermore National Laboratory with other laboratory and university collaborators wherein a 3 m × 3 m × 4.5 m block of rock was studied as it was heated from ambient temperatures to approximately 145°C. The purpose of the test was to study coupled thermal, hydrological, chemical, and mechanical processes in response to heating at a scale significantly larger than that possible in laboratory studies. Detailed descriptions of the test design, instrumentation, results and interpretation, and relevance to the nuclear waste isolation program can be found in numerous reports (e.g., Wilder et al., 1997; Lin et al., 1998). The LBT provides a unique opportunity to evaluate the use of electrical resistance tomography and laboratory measurements to determine saturation and to detect fractures in a rock similar to many geothermal reservoirs. To that end, key points of the LBT relating to this effort are repeated here.

An outcrop area at Fran Ridge, Nevada, was selected to be the site for the LBT because of the suitable rock type exposed and accessibility of the site. The block of fractured non-lithophysal Topopah Spring tuff was isolated and excavated, and the fractures on five sides of the block were mapped in detail. Figure 1 shows the block, partially exposed for fracture mapping, prior to installation of test and monitoring instrumentation. Instruments and heaters were installed within and on the surface of the block. The instruments installed in the block included resistance temperature devices (RTD) to measure temperatures, electrodes to conduct electrical resistivity tomography (ERT), Teflon liners for neutron logging in boreholes, Humicaps to measure relative humidity, pressure transducers to measure gas-phase pressure, conventional and optical multiple-point borehole extensometers (MPBX) for measuring displacements along boreholes, and fracture gauges mounted across fractures on the block surface to monitor fracture deformation. To create a one-dimensional thermal field within the block heaters were placed in the rock 1.75 m from the base to simulate a plane heat source, and an aluminum plate fitted with heating/cooling coils was mounted on the top of the block. This plate was connected to a heat exchanger to allow thermal control of the top surface at approximately 60°C. The heaters generated 450 W each and were installed in each of the five horizontal heater holes. The heaters were turned on on February 28, 1997, and turned off on March 10, 1998. Data continued to be collected until September 30, 1998 as the rock mass cooled.

PLACE FIGURE 1 HERE

FIELD EXPERIMENTAL PROCEDURES

ERT is a geophysical imaging technique that can be used to map subsurface resistivity (Daily and Owen, 1991). ERT measurements at the LBT were performed by Ramirez and Daily

(2000)—their procedures for data collection and inversion are outlined here. The ERT measurements consist of a series of voltage and current measurements from buried electrodes using an automated data collection system. The data are then processed to produce electrical resistivity tomographs that can be used to infer changes in water content, temperature, and fluid chemistry. ERT was proposed as a geophysical imaging tool by Lytle and Dines (1978). Early adaptations of the technique to the field of geophysics were by Pelton et al. (1978), Dines and Lytle (1981), Tripp et al. (1984), Wexler et al. (1985), Oldenburg and Li (1994), Sasaki (1992), Daily and Owen (1991), and LaBrecque et al. (1996b).

The important features of the two-dimensional (2D) algorithm used for ERT are described here. The algorithm (see LaBrecque et al., 1996a) solves both the forward and inverse problems. The forward problem is solved using a finite element technique in two dimensions. The inverse problem implements a regularized solution that minimizes an objective function. The objective of the inverse routine is to minimize the misfit between the forward modeling data and the field data, and a stabilizing functional of the parameters. The stabilizing functional is the solution roughness. The inversion routine attempts to find the smoothest resistivity model that fits the field data to a prescribed tolerance. Resistivity values assigned in this way to the finite element mesh constitute the ERT image. Although the mesh is of a large region around the electrode arrays, only the region inside the ERT electrode array is used in the calculations of moisture content and reported here because the region outside the array is poorly constrained by the data.

To calculate changes in the electrical resistivity we compared a data set obtained after heating started, and a corresponding set obtained prior to heating. One may consider subtracting, pixel by pixel images from these two different conditions. However, this approach could not be used because the resistivity structure is three-dimensional. The finite element forward solver, constrained to 2-D, cannot generate a model that adequately fits the data. Our experience is that these effects can be reduced by inverting the quantity

$$r_a/r_b \times r_h \quad , \tag{1}$$

where r_a is the measured transfer resistance after heating started, r_b is the transfer resistance before heating, and r_h is the calculated transfer resistance for a model of uniform resistivity. This approach tends to reduce the effects of anomalies which do not satisfy the 2D assumptions of the resistivity model, because the 3D effects tend to cancel in the ratio since they are contained in both terms r_a and r_b.

From the resulting changes in resistivity, changes in saturation can also be determined using laboratory resistivity data as described below. ERT images were taken every four to six weeks during the course of the LBT.

LABORATORY EXPERIMENTAL PROCEDURES

Experimental Apparatus

A complete description of the experimental apparatus and measuring procedures was reported by Roberts et al. (2001a). The apparatus consists of an externally heated pressure vessel with separate pumps and controls for confining pressure and pore pressure on either side of the sample (Fig. 2). Pore pressure was controlled independently between 0 and 5.0 MPa and, for convenience, the two systems are referred to as up- and down-stream pressure systems. An impedance bridge was used to measure the resistance of the electrically isolated samples at

1 kHz. Electrical resistivity was calculated from the resistance and geometry of the core. Temperature was measured with type T thermocouples with an accuracy of ±2°C. Resistivity measurements have been made at temperatures up to 275°C, but for this study were limited to 145°C, the highest temperature of the LBT field experiment. Data collection was automated by use of a scanning unit and microcomputer.

PLACE FIGURE 2 HERE

Samples and Preparation

Samples were procured from the LBT site and characterized. The sample porosity ranged between 8 and 20%, with an average porosity of 11.5 ± 0.02%, as determined by mercury injection porosimetry (Carlberg and Roberts, 2000). The samples used for the electrical properties measurements here had porosities of ~11-13% as determined by subtracting dry density from wet density (Roberts, 2001). Samples were prepared by machining right-circular cylinders approximately 2.0 cm high and 2.5 cm in diameter. Samples were saturated with a pore fluid prepared from high-purity salts and distilled water (1.65 g NaCl per liter of water) by taking samples dried under vacuum at 35°C and back-filling with the NaCl solution. Samples were then left immersed in the solution for several days until the weights were constant, indicating that saturation was complete. The saturating fluid was boiled for one hour before being used for saturating the samples to remove dissolved gases. The fluid was also pumped under rough vacuum for about 2 hours for more complete gas removal. Fluid resistivity at room temperature was ~6.4 Ω-m (conductivity = 1.57 mS/cm). Details regarding the sample assembly and electroding are described in Duba et al. (1997).

Cylindrical samples containing artificial fractures were prepared by cutting the samples in half lengthwise and regrinding the two halves to a cylindrical shape. The fractures were created by grinding a slot the entire length of one half of the sample. The dimensions of the slot were 0.5 × 20 × 19 mm for a volume of ~0.19 cm^3 and the total volume of the sample is ~10.2 cm^3. The slot was supported by ridges of rock left in place at the edges of the sample so that the slots remained open during experiments. The two halves were ground flat and, when mated, only the slot permitted the free passage of fluid.

ELECTRICAL RESISTIVITY RESULTS AND DISCUSSION

Resistivity of Tuff as a function of Saturation and Temperature

The resistivity of intact tuff from the LBT site and tuff from nearby sites has been measured (Roberts and Lin, 1997; Roberts, 2001). Typical results are shown in Fig. 3 where it can be seen that saturation has a strong effect on resistivity, with the strongest saturation dependence between 0 and 40% saturation. The dependence on saturation is still strong up to 100% saturation, although this is not apparent on the semi-log plot. For all samples and saturations, and temperatures up to 95°C, the temperature dependence of conductivity at a given saturation follows an Arrhenius relationship,

$$\sigma = \sigma_o \exp(-Ea/kT) \quad , \qquad (2)$$

where T is temperature, k is the Boltzmann constant ($k = 1.381 \times 10^{-23}$ J/K), Ea is the activation energy, and σ_o is a pre-exponential term. Equation (2) was used to fit each saturation level.

Additional measurements on a fully saturated tuff sample from the LBT (Tptlg) in the high-temperature, high-pressure device up to 145°C indicate a similar temperature dependence. In all cases the activation energy for conduction is between 0.15 and 0.28 eV with the activation energy negatively correlated with saturation (Roberts, 2001). An activation energy of 0.13 to 0.20 eV describes the temperature dependence of the viscous flow of water (Llera et al., 1990) and is evidence that, in these samples, the majority of conduction is through an aqueous ionic diffusion process.

Effects of Fractures on Resistivity

Resistivity as a function of pore pressure for samples Tptlg (intact) and Tptlgs (slotted) are shown in Fig. 4. The confining pressure was held constant at 3.56 MPa while the pore pressure varied. These starting pressures are such that the confining pressure:pore pressure ratios are approximately 2:1. Previous studies showed that confining pressure has a minimal effect on the electrical properties of intact rocks of this type at these conditions (Llera et al., 1990; Duba et al., 1997).

The resistivity ratio (of the fractured sample to the intact sample) is less than one in the liquid region (to the right of the vertical line on Fig. 4). This ratio is greater than one to the left of the vertical line (the boiling region; Haas, 1971). The addition of the fracture lowers the resistivity by providing a conductive pathway when filled with liquid water. This parallel conductor has a large effect on intermediate porosity material, such as welded tuff.

The data indicate several notable features. Considering the intact sample, the electrical properties are similar to previous results (Roberts et al., 2001a) in that as the pore pressure is lowered little change in resistivity occurs until the boiling pressure is reached. At this point resistivity gradually increases as the pore pressure is lowered further. The interpretation is that capillary forces in the smaller pores maintain the fluid in the liquid state. Both the samples studied here exhibit this behavior.

As the pore pressure is lowered below the boiling point of bulk water there is no immediate increase in the resistivity of the intact samples as a result of vapor-pressure lowering. The fractured sample shows a resistivity increase as soon as the pore pressure is equal to the boiling pressure. At this pressure the resistivities of the intact and fractured samples cross, with the fractured sample suddenly significantly more resistive than the intact sample. A large resistivity change at the boiling pressure is expected because there is essentially no capillary suction in the relatively large-size slot. Another interesting aspect of the two types of samples is that the higher resistivity increases as pore pressure is lowered further. The most likely explanation is that more intact rock surface is exposed to the lower pressure so that more pores can easily lose water to the fracture. This creates a higher resistivity region adjacent to the fracture. Thus, when considering fracture location in a reservoir using electrical methods, accessible fractures that have large exposed surface areas would be expected to show greater resistivity changes upon drying or resaturation. This is the case in the study of the LBT.

RESULTS FROM THE LARGE BLOCK TEST

Determination of Saturation Changes

Using the laboratory electrical data and the inversions of resistivity change in response to heating at the LBT, we have attempted to estimate saturation changes in the matrix of the host rock. To do so we constructed a petrophysical model of resistivity vs saturation for temperatures between 15 and 200°C (Fig. 5). One assumption of the model is that for saturations above ~20% the Arrhenius relation (Eq. 2) applies. It was determined based, on the laboratory data, that at low saturations (below ~20%) the dependence of resistivity on saturation followed an exponential:

$$\rho = \rho_o \exp(CSw) \quad , \tag{3}$$

where ρ is the resistivity, ρ_o is the resistivity at zero saturation, C is the slope, and Sw is the saturation. Equation 3 was implemented into the model for saturations below 20%. This change in dependence of resistivity at saturations near 20–30% indicates a fundamental change in the dominant conduction mechanism. Roberts and Lin (1997) attribute this to an increase in the contribution of surface conduction to total conduction at very low saturation. An additional assumption is that the initial saturation of the matrix is 75% (Wilder et al., 1997; Ramirez and Daily, 2000). The fitting parameters σ_o and Ea from Equation 2 were averaged for all laboratory data sets. The resulting set of curves (Fig. 5) agree well with the laboratory data and vary predictably enough to convert the ERT resistivity ratios to saturation ratios.

Fracture Detection Using Electrical Methods

Geophysical imaging methods that use galvanic or inductive currents to probe for fractures depend on detecting contrasts in resistivity (anomalies) associated with the fractures. These resistivity anomalies depend on fracture density and aperture, resistivity of the fluid filling fractures and pores, and the electrical properties of the rock matrix. The resistivity changes and calculated saturation changes in Fig. 6 show several very interesting features. The seven images cover approximately six months of the test. The most notable feature is the dry-out region at the level of the heaters where the temperature has increased the most. Another pronounced feature is the large increase in resistivity in the upper left (west) portion of the block. This feature gradually develops and persists throughout the duration of the test and is suggestive of a hydraulically connected fracture or fracture network that has allowed moisture to escape with subsequent dryout of the adjacent matrix.

A similar, but less pronounced, feature began to develop on the upper eastside of the block (top right of image) around May 22, 1997. This feature is also suggestive of dry-out along a fracture and progressively shows less saturation until August 26, 1997. On this date the saturation of the region has changed, indicating re-wetting rather than dryout. The last image shows the rock drying in a slightly different location. The MPBX indicate rapid displacement that may indicate movement along fractures in that part of the block. The data suggest that only fractures in one area moved, the eastern part of the block, just six days before the August 26 ERT survey (Fig. 6). Temperature data from a nearby borehole indicate a drop in temperature from ~110°C to 98°C (boiling) on the same day as the fracture movement. This is further evidence of a coupled thermal–hydrological event that was clearly captured by the ERT.

CONCLUSIONS

Laboratory measurements of electrical resistivity were performed on representative geothermal reservoir rocks. Measurements on intact rocks as functions of saturation and temperatures up to 145°C were used to calculate saturation changes in a $3 \times 3 \times 4.5$ m heated rock mass. The resulting constitutive model permits the prediction of electrical resistivity at temperatures up to 200°C. Measurements on rocks with synthetic propped fractures reinforce the idea that electrical measurements provide a means for fracture detection. The resistivity contrast during boiling appears to be relatively insensitive to fracture aperture but increases with accessible fracture surface area.

The time-lapse field ERT measurements at the Large Block Test were used in combination with a laboratory-derived model to image dynamic saturation changes. The results were confirmed by comparing with saturations determined by independent geophysical tests such as neutron logging. Fractures can be detected by locating the regions of highest resistivity contrast. The time dependence of the resistivity contrast is useful for monitoring fluid migration from fractures into the matrix. In the case of the LBT a rewetting episode attributable to mechanical displacement of a fracture was observed. These results are applicable to fracture detection in other rock types and other field areas.

ACKNOWLEDGMENTS

S. Fletcher and C. Talaber provided essential technical support and expertise. We thank P. Kasameyer for fruitful discussion and comments. This work was supported by the Office of Wind and Geothermal Technology, under the Assistant Secretary for Energy Efficiency and Renewable Energy of the U.S. Department of Energy, and the Office of Basic Energy Science and was performed by Lawrence Livermore National Laboratory under Contract W-7405-Eng-48.

REFERENCES

Carlberg, E. D., and J. J. Roberts (2000), Microstructural analyses of Topopah Spring Tuff from the Large Block Test at Fran Ridge, Nevada, *UCRL-ID-137110*, Lawrence Livermore National Laboratory, Livermore, CA.

Daily, W. and E. Owen (1991), Cross-borehole resistivity tomography, *Geophysics, 56,* 1228-1235.

Duba, A., Roberts, J. J., and Bonner, B. P. (1997), Electrical properties of geothermal reservoir rocks as indicators of porosity distribution, *Proceedings Twenty-second Annual Stanford Geothermal Reservoir Engineering Workshop*, 383-389.

Haas, J. L. Jr. (1971), The effect of salinity on the maximum thermal gradient of a hydrothermal system at hydrostatic pressure, *Economic Geol., 66*, 940-946.

LaBrecque, D. J., Miletto, M., Daily, W., Ramirez, A., and Owen, E. (1996a), The effects of noise on Occam's inversion of resistivity tomography data, *Geophysics*, *61*, 538-548.

LaBrecque, D. J., A. Ramirez, W. Daily, A. Binley and S. Schima (1996b), ERT monitoring of environmental remediation processes, *Meas. Sci. Technol., 7,* 375-383.

Lin, Wunan, D. Wilder, S. Blair, W. Daily, G. Gdowski, W. Glassley, K. Lee, A. Meike, A. Ramirez, J. Roberts, D. Ruddle, J. Wagoner, D. Watwood, T. Williams, R. Carlson, and D. Neubauer (1998), An overview of progress on the Large Block Test, *International High Level Waste Conference, UCRL-JC-128796*, Lawrence Livermore National Laboratory, Livermore, CA.

Llera, F. J., Sato, M., Nakatsuka, K., and Yokoyama, H. (1990), Temperature dependence of the electrical resistivity of water-saturated rocks, *Geophysics, 55*, 576-585.

Lytle, R. J. and K. A. Dines (1978), An impedance camera: A system for determining the spatial variation of electrical conductivity, *UCRL-52413*, Lawrence Livermore Laboratory, Livermore, California,.

Oldenburg, D. W. and Y. Li (1994), Inversion of induced polarization data, Geophysics, vol. 59, no. 9, pp 1327-1341.

Pelton, W. H., L. Rijo and C. M. Swift, Jr. (1978), Inversion of Two-dimensional resistivity and induced-polarization data, *Geophysics, 43*, no. 4, 788-803.

Ramirez, A. and Daily, W. (2000) "Electrical Imaging at the Large Block Test-Yucca Mountain, Nevada," *submitted to J. App. Geophy.*, also Lawrence Livermore National Laboratory Report, UCRL-JC-140906.

Roberts, J. J. (2001), Electrical properties of Topopah Spring tuff as a function of saturation and temperature, *J. Geophys. Res., submitted*, also Lawrence Livermore National Laboratory Report, UCRL-JC-142099.

Roberts, J. J., Bonner, B. P., and Duba, A. G. (2000), "Electrical Resistivity Measurements of Andesite and Hydrothermal Breccia from the Awibengkok Geothermal Field, Indonesia," *Twenty-Fifth Annual Stanford Geothermal Reservoir Engineering Workshop*, 339-344.

Roberts, J. J., Bonner, B. P., and Kasameyer, P. W. (2001a), Electrical resistivity measurements of intact and fractured geothermal reservoir rocks, *Proceedings Twenty-Sixth Annual Stanford Geothermal Reservoir Engineering Workshop* (in press).

Roberts, J. J., A. G. Duba, B. P. Bonner, and P. Kasameyer (2001b), The effects of capillarity on electrical resistivity during boiling in metashale from scientific corehole SB-15-D, The Geysers, California, USA, *Geothermics, 30*, 235-254.

Roberts, J. and W. Lin (1997), Electrical properties of partially saturated Topopah Spring Tuff: Water distribution as a function of saturation, *Water Res. Research, 33*, No. 4, 577-587.

Sasaki, Y. (1992), Resolution of resistivity tomography inferred from numerical simulation, *Geophysical Prospecting, 40*, 453-463.

Tripp, A. C., G. W. Hohmann and C. M. Swift (1984), Two dimensional resistivity inversion, *Geophysics, 49*, 1708-1717.

Wexler, A., B. Fry and M. R. Neuman (1985), Impedance-computed tomography algorithm and system, *Applied Optics, 24*, no. 23, 3985-3992.

Wilder, D., W. Lin, S. C. Blair, T. Buscheck, R. C. Carlson, K. Lee, A. Meike, A. L. Ramirez, J. L. Wagoner, and J Wang (1997), Large Block Test status report, *UCRL-ID-128776*, Lawrence Livermore National Laboratory, Livermore, CA, Chapter 2, page 20.

This work was performed under the auspices of the U.S. Department of Energy by the University of California, Lawrence Livermore National Laboratory under Contract No. W-7405-Eng-48.

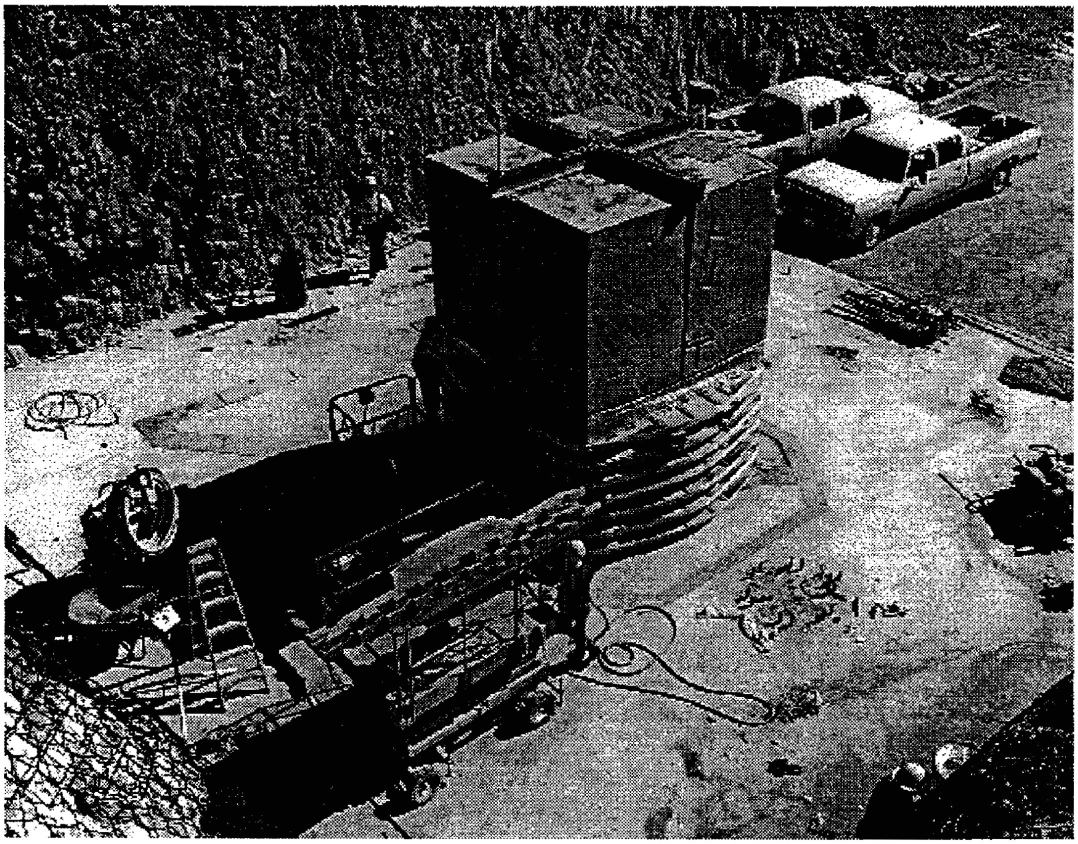

Figure1. The Large Block Test at Fran Ridge, Nevada.

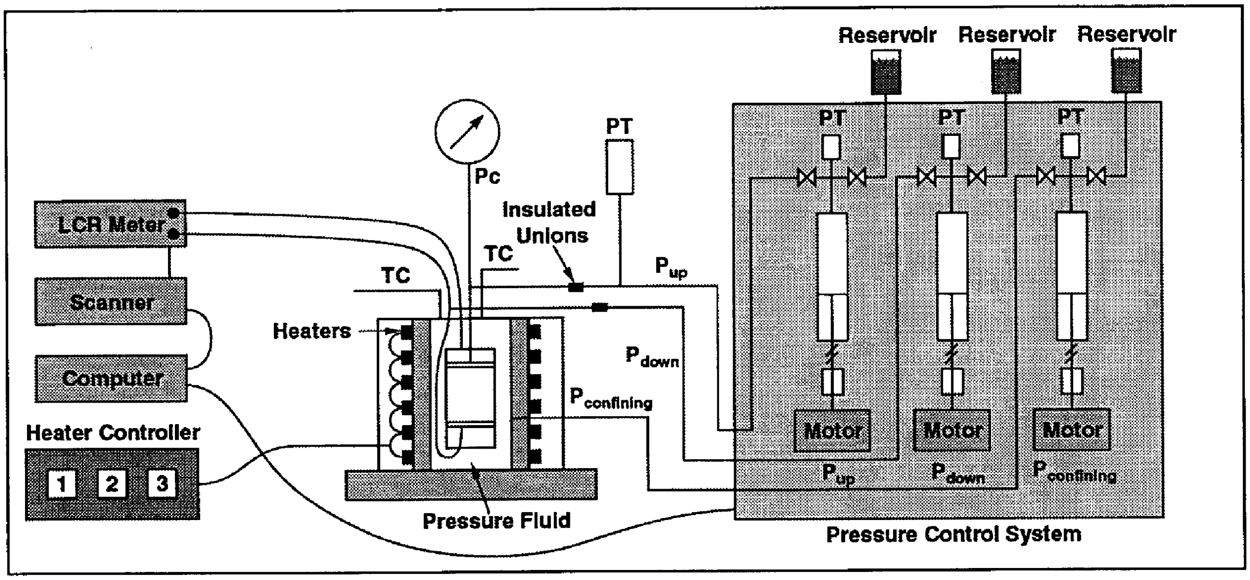

Figure 2. Schematic of apparatus. Sample is electrically isolated and held in an externally heated pressure vessel with separate reservoirs, pumps, and controls for confining and pore pressure. Type T thermocouples measure temperature of the three-zone heater and at two locations adjacent to the sample. An impedance bridge (LCR meter, HP4284A) is used to measure the electrical properties of the sample. A microcomputer controls the experiment and data collection.

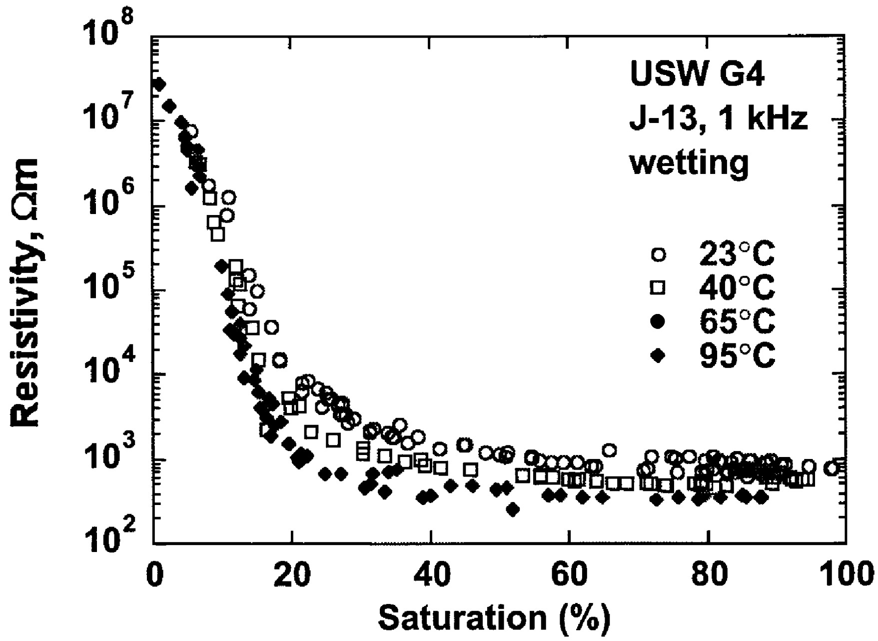

Figure 3. Resistivity vs saturation for tuff sample USW G4 during wetting at 23, 40, 65, and 90°C (filled circles, open squares, open diamonds, and filled diamonds, respectively).

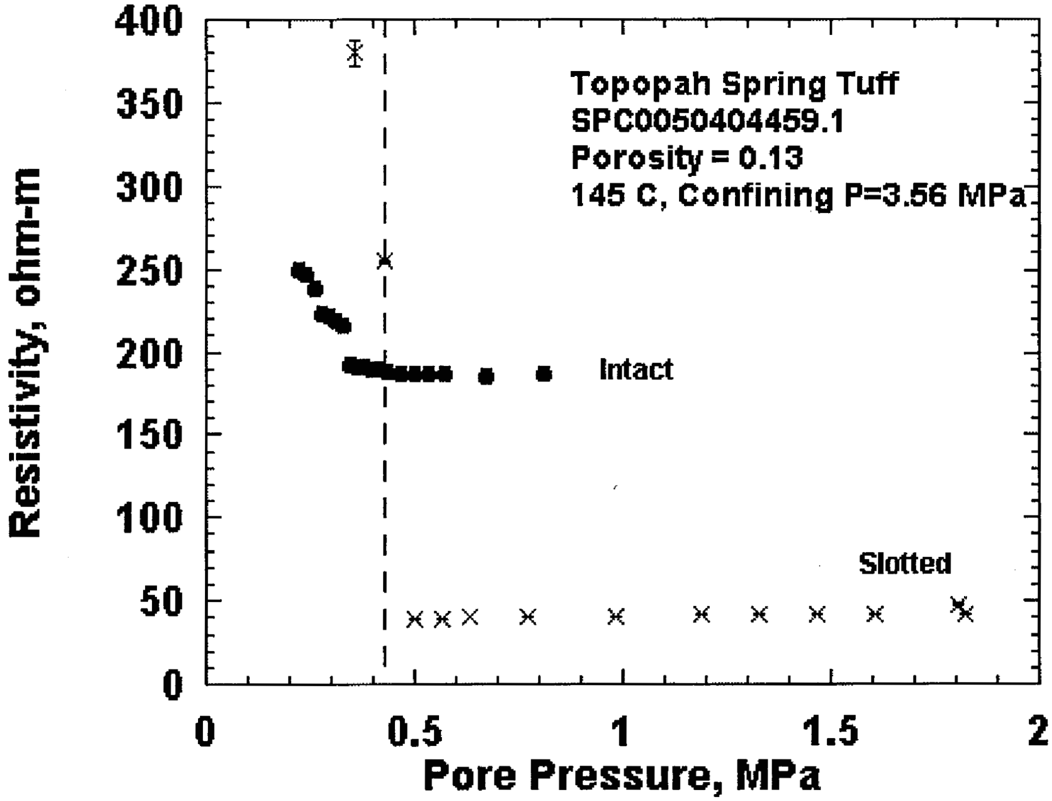

Figure 4. Resistivity vs pore pressure for tuff sample Tptlg at 145°C (intact sample, circles, fractured sample, crosses). Confining pressure was held constant while the pore pressure was changed. The vertical line indicates the boiling pressure for water at 145°C.

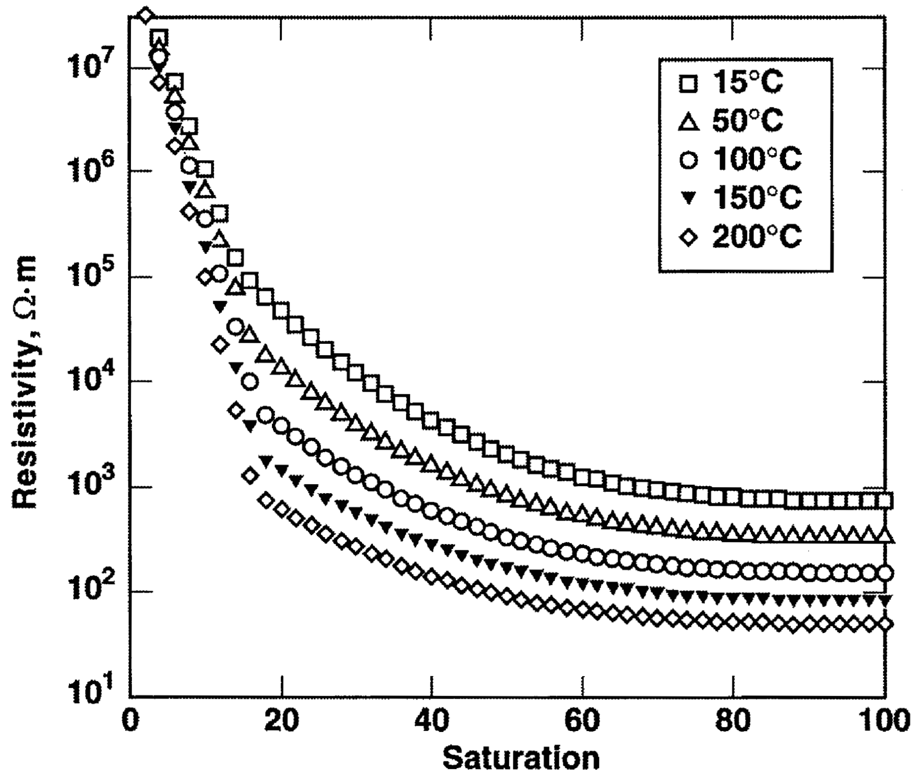

Figure 5. Resistivity vs saturation model used to calculate saturation changes based on the ERT inversions. The Arrhenius relation (Eq. 2) was used to predict resistivity at saturations above ~20% and equation 3 was used at saturations below ~20%. This approach provided the best agreement with the laboratory data for all temperatures and saturations.

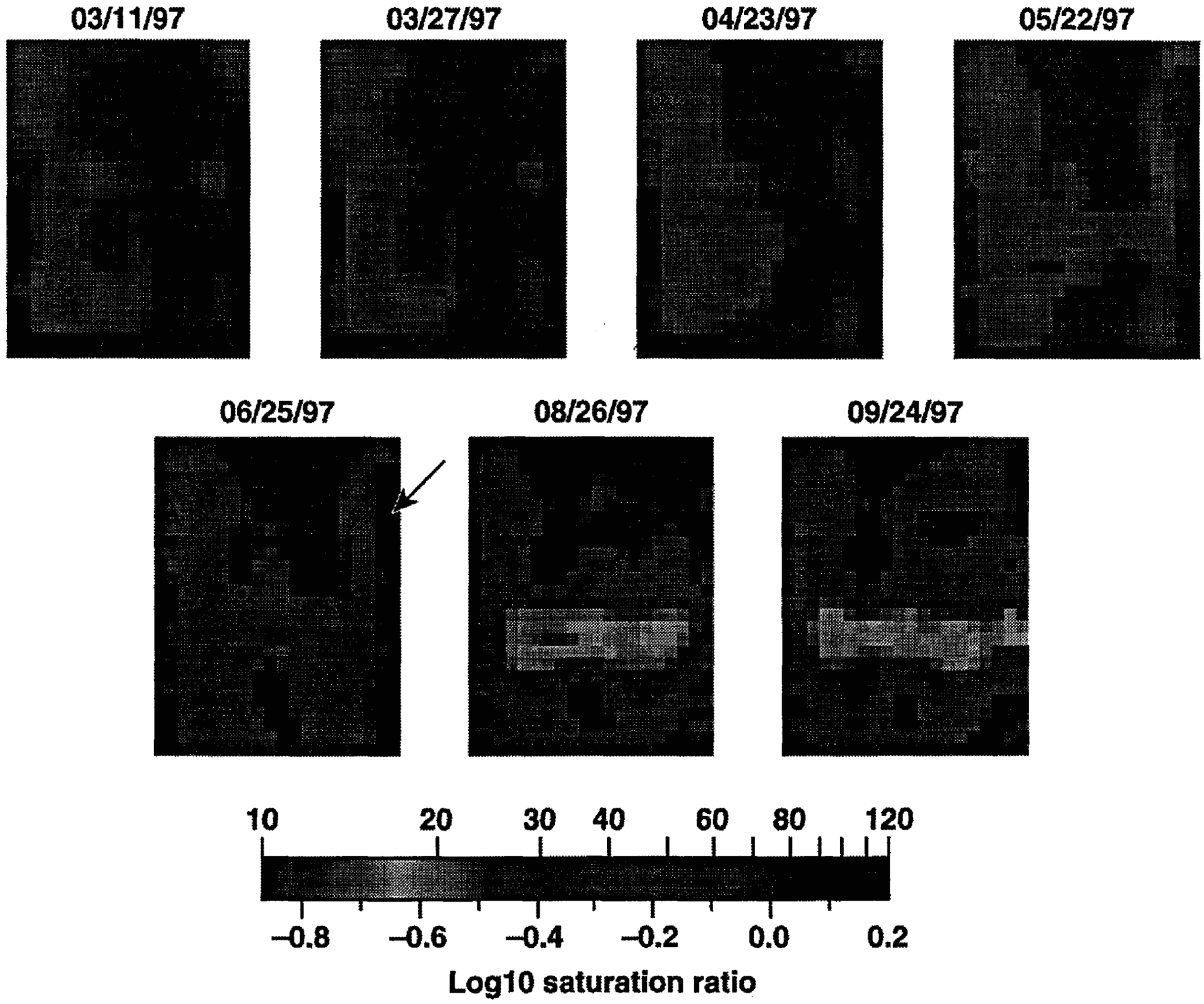

Figure 6. ERT images of saturation in the LBT as a function of elapsed time (indicated above each image). Initial saturation was assumed to be 75%. Heater horizon is about 1/3 from the bottom of the images and is the region displaying the most dryout. Arrow on 06/25/97 image indicates drying fracture that rewet by 08/26/97.

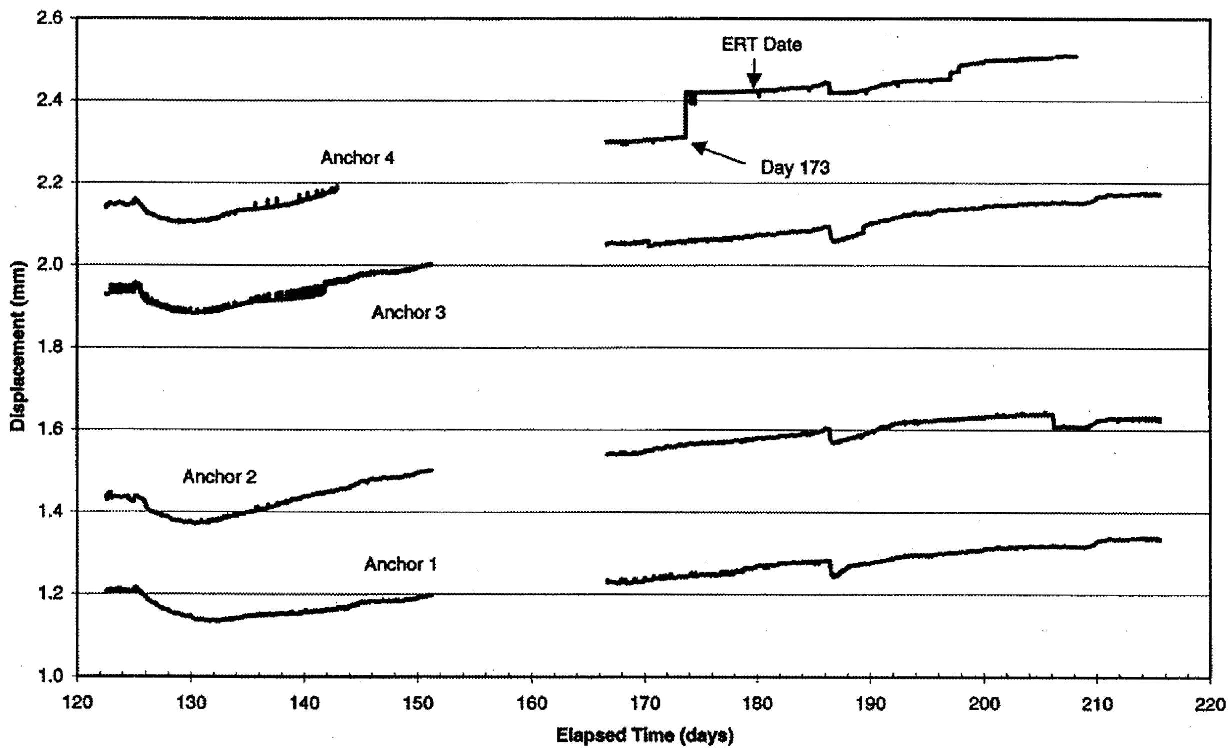

Figure 7. Displacement as a function of time for four MPBX anchors near the top of the LBT. Anchor 1 was on the west side of the block and anchor 4 on the eastern side of the block. The ERT image taken August 26, 1997(day 180) occurred just after movement was detected between anchors 3 and 4. The saturation in the top, eastern part of the block indicates rewetting of a fracture and the matrix (Fig. 5).